Published May 1, 1992

The Extent of Clonal Structure in Different Lymphoid Organs

By Mirjam H. A. Hermans,*‡ Auk Wubbena,* Frans G. M. Kroese,* Simon V. Hunt,§ Richard Cowan,‖ and Davina Opstelten*‡

*From the *Department of Histology and Cell Biology, Immunology Section, University of Groningen, 9713 EZ Groningen, The Netherlands; the ‡Department of Biochemistry, University of Hong Kong, Hong Kong; §Sir William Dunn School of Pathology, University of Oxford, Oxford OX1 3RE, United Kingdom; and the ‖Department of Statistics, University of Hong Kong, Hong Kong*

Summary

To gain insight into the clonal organization of lymphoid organs, we studied the distribution in situ of donor-derived cells in near-physiological chimeras. We introduced $RT7^b$ fetal liver cells into nonirradiated congenic $RT7^a$ neonatal rats. The chimerism 6–20 wk after injection ranged from 0.3 to 20%. The numbers of cell clones simultaneously contributing to cell generation in a particular histological feature were deduced from the variance in donor cell distribution. In bone marrow and thymus, donor-derived lymphoid cells were found scattered among host cells, indicating a high mobility of cells. In bone marrow, donor cells were evenly distributed over the entire marrow, even at low chimerism. This indicates that leukopoiesis is maintained by the proliferation of many clones. In the thymus, the various lobules showed different quantities of donor-derived lymphoid cells. Mathematical analysis of these differences indicated that 17–18 cell division cycles occur in the cortex. In spleen, the distribution of donor-derived cells over the germinal centers indicated that 5 d after antigenic stimulation, germinal centers develop oligoclonally. The main conclusions of this work are that (*a*) bone marrow and thymus are highly polyclonal; (*b*) 17–18 divisions occur between prothymocyte and mature T cell; and (*c*) lymphoid cells disperse rapidly while proliferating and differentiating.

By proliferation and differentiation from pluripotent hemopoietic stem cells to lymphocytes, cell populations with highly diverse antigen-receptor specificities are generated and maintained. To understand this generation of the antigen-receptor repertoire, a better insight into the clonal organization of the lymphoid system is required. Particularly relevant issues are the numbers of B and T lymphoid cell clones (a clone is the progeny of a single ancestor cell) that simultaneously contribute to the generation of lymphocytes, the size and antigen receptor composition of individual clones, and the nature of the interactions of the progeny cells with the environment. To study the number of clones simultaneously engaged in production of hemo/lymphopoietic cells, chimeric animals are used since genotypic fluctuations in these animals are an indication for progenitor cell numbers.

In bone marrow (BM),[1] hemopoietic cells, including B lymphocytes, are generated. Reports so far have described hemopoiesis to be mono- or oligoclonal (1–5), and/or polyclonal (3, 5–7). Analysis of individual clones indicated that some clones contribute temporarily to one or more lineages of hemopoiesis, while others do so continuously (8–11). In the spleen, Peyer's patches, and other lymphoid organs, B lymphocytes expand in germinal centers (GC): histologically defined groups of B lymphoid blasts that arise after stimulation with antigen. Splenic GC develop oligoclonally, from a few GC precursor cells (12–14). Cells from BM home toward and populate the thymus where they expand and give rise to functional T lymphocytes (15). As for BM, reports on the clonal structure of the thymus vary, from an oligoclonal (16–19) to a polyclonal (20) development of thymocytes.

We investigated the clonal structure of the lymphoid system by in situ analysis of near-physiological chimeras. We introduced fetal liver (FL) cells into nonirradiated neonatal recipients to produce a wide range of degrees of chimerism. FL, rather than BM, was used as a stem cell source because of its relatively high content of stem cells with a high self-renewal capacity (21–25). RT7 (CD45, L-CA) served as a marker because of its wide, but also exclusive, hemopoietic distribution (26) and its detectability in single cells. To minimize influence of the genetic marking on the clonal development of the hemopoietic cells, we used RT7 congenic rats.

From the results we conclude that: (*a*) hemopoiesis and thymopoiesis are maintained by the activity of a large number of simultaneously active clones; (*b*) in the thymus a cell di-

[1] *Abbreviations used in this paper:* BM, bone marrow; FL, fetal liver; GC, germinal centers; NCS, newborn calf serum; TRITC, tetramethylrhodamine isothiocyanate.

 J. Exp. Med. © The Rockefeller University Press • 0022-1007/92/05/1255/15 $2.00
Volume 175 May 1992 1255–1269

vides about 18 times while it matures; and (*c*) lymphoid cells in BM and thymus move from one microenvironment to the other while they develop.

Materials and Methods

Animals

PVG RT7^b congenic rats derived by 12 generations of backcrossing to PVG (27) were from stocks held at the Department of Histology and Cell Biology, University of Groningen, and at the Sir William Dunn School of Pathology, University of Oxford, and maintained under conventional conditions. The two known alleles, RT7^a and RT7^b (28), encode the RT7.1 and RT7.2 alloantigens, respectively. In this paper, RT7^a and RT7^b refer to the genotype of the cells, while RT7.2 refers to the (protein) product of the RT7^b gene, as detected with the anti-RT7.2 mAb HIS41.

Construction of Hemopoietic Chimeras

Timed matings were scored daily by vaginal smearing (appearance of sperm in smear = day 0). Livers were removed from day 14–16 fetuses and thoroughly suspended by physical disruption through a Pasteur pipette in RPMI 1640 (Gibco Europe, Glasgow, Scotland) supplemented with 10% FCS (Gibco Europe). Large particles were removed by 1 *g* sedimentation into 1 ml newborn calf serum (NCS; Gibco Europe) for 5 min on ice. The FL cells in the upper layer were then centrifuged through 1 ml NCS (10 min, 200 *g* 4°C) and resuspended in RPMI/FCS. The cell yield varied from 4.6 to 7.2 × 10^6 cells per embryo. Within 24 h after birth or at the age of 5 d, RT7^a rats were anesthesized by hypothermia and received a single injection of RT7^b FL cells (0.6–8.4 × 10^7 cells) intraperitoneally, in a volume of 100 μl using a 1-ml syringe fitted with a 30-gauge needle. There was a peritoneal leak for one rat (out of 10 injected) immediately after injection; this rat was not included in Fig. 1.

Induction of GC in Spleen

To induce GC formation in the spleen, 10^9 SRBC were injected intravenously in 9-wk-old chimeric rats; the rats were killed 5 d later.

Antibodies

First-stage antibodies are listed in Table 1. Anti-TdT was from Supertechs Inc. (Bethesda, MD) and W3/13 (antileukosialin) and anti-rat μ chain was from the Sir William Dunn School of Pathology, University of Oxford. In rat BM, W3/13 labels most of the myeloid lineage strongly, T cells and plasma cells strongly, and some erythroid cells and early lymphoid cells weakly (30, 36). ED2 was a kind gift of Dr. C. Dijkstra (Free University, Amsterdam, The Netherlands). mAb MARD-3 was a kind gift from Dr. H. Bazin (University of Louvain, Brussels, Belgium). HIS8, HIS40, HIS41, HIS49, HIS50, and HIS51 were from the Department of Histology and Cell Biology, University of Groningen, Groningen.

Second-stage antibodies: goat anti-rabbit Ig (H+L) conjugated to tetramethylrhodamine isothiocyanate (TRITC) or FITC, goat anti-mouse-γ1-FITC and TRITC, goat anti-mouse-γ2a-FITC, and goat anti-mouse-γ2b-FITC were from Southern Biotechnology Associates (Birmingham, AL). Polyclonal peroxidase-conjugated rabbit anti-mouse Ig(H+L) antibody was from Dakopatts (Glostrup, Denmark). Second-stage antibodies were diluted to the appropriate working dilution with PBS containing 2–5% (vol/vol) normal rat serum. Just before use, all antibodies were centrifuged at 15,000 *g* for 15 min to remove aggregates.

Tissue and Cell Staining Procedures

BM. Two femurs and two tibias were cut transversally into two halves. The part proximal to the knee joints was prepared for histology as detailed elsewhere (35). The other halves of the bones were flushed to make cell suspensions, pooled, cytocentrifuged, and fixed as described (36). Indirect immunofluorescence procedures were performed as described (37). In single-staining procedures, FITC was used. In double-staining procedures (HIS41 in combination with other markers), HIS41 was detected with a TRITC-conjugated second-stage antibody and the other markers with FITC. Preparations were mounted in Citifluor (Citifluor, London, England) to prevent fading of fluorescence.

Non-BM Tissues. FL cells were prepared as described above, cytocentrifuged, fixed, and stained. Other tissues were snap frozen in liquid freon, and 7-μm thick sections were cut in a cryostat (Bright Instrument Company Ltd., Huntingdon, UK). Each spleen was cut in three parts, which were frozen, and sets of serial frozen sections were cut transversally at well separated levels (minimally 300-μm distant from each other). Sections from spleen and thymus were fixed in acetone and stained using an indirect immunoperoxidase technique (38).

In all staining procedures controls were included to check for crossreactivity of second-stage antibodies against rat Ig, other substances, or other mouse Ig isotypes.

Microscopic Analysis of Tissues and Cell Suspensions

Immunostained sections of BM, spleen, and thymus were used to analyze the distribution pattern of donor cells. For BM and FL, quantitative data were obtained by cytocentrifugation of suspended cells and subsequent fixation and staining. Preparations were examined using a fluorescence microscope (E. Leitz, Inc., Rockleigh, NJ) as described (35). Unless stated otherwise, the number of cells analyzed was such that at least 100 cells of the least abundant cell type were scored.

Photography

Fluorescence photographs were made using a diaplan microscope (E. Leitz, Inc.), equipped with filter sets for selective observation of FITC and TRITC emission, and an Orthomat E camera. Ektachrome 400 ASA film was used, exposed at 400 ASA for FITC and 1600 ASA for TRITC. Peroxidase stained sections were photographed in an axiophot microscope (Carl Zeiss, Inc., Thornwood, NY) using Ektachrome 50 ASA film.

Analysis of Thymus Sections

To draw the distinction between medullary and cortical areas, a complete thymus section was photographed under darkfield illumination using a 6.3× objective and 10× ocular (~35 photographs per section). The correctness of the demarcation lines between cortex and medulla drawn was checked under the microscope using phase contrast illumination and a 40× objective.

To determine the frequencies of lymphoid (≤8 μm in size, stained all around the cell in a smooth, regular pattern) HIS41$^+$ cells in all lobules (lobule = area of thymic tissue that was completely surrounded by septa and/or capsule in the plane of section, see Fig. 5) of each thymus section, phase contrast photomicrographs (×503) were made. For analysis of the cortex, within regularly shaped lobules, four photomicrographs, each representing an area of 0.044 mm^2, were taken (one north, one west, one south, and one east, see Fig. 5). If the size of the lobule was too small for four photographs, fewer photographs were taken, and if a lobule was relatively large and irregularly shaped, more photographs were taken.

Published May 1, 1992

Table 1. *List of mAbs against Rat Antigens Used in This Study*

Antibody	Species, isotype	Reference	Specificity in rat
Anti-TdT	Rabbit, polyclonal		TdT
Anti-rat μ	Rabbit, polyclonal	29	Ig μ chain
W3/13	Mouse, IgG1	30	CD43; in BM: a marker for myeloid cells (see Materials and Methods)
ED2	Mouse, IgG2a	31	Macrophages
MARD-3	Mouse, IgG1		Ig δ chain
HIS40	Mouse, IgG1	32	Ig μ chain
HIS8	Mouse, IgG1	33	Ig κ chain
HIS41	Mouse, IgG1, IgG2b	34	CD45; rat RT7.2 allotype of L-CA
HIS49	Mouse, IgM	35	Erythroid cells
HIS50	Mouse, IgM	Hermans et al., manuscript in preparation	B lymphoid cells
HIS51	Mouse, IgG2a	35	Thy-1

In each photograph an area containing at least 100 HIS41$^+$ cells was analyzed. For analysis of the medulla, depending on the size of the medulla, at most four (n, w, s, e) photographs were taken, each of which analyzed as described for the cortex, except for the total number of HIS41$^+$ lymphoid cells analyzed, which in this case varied from 42 to 92 per photograph. To determine the average total number of nucleated cells in cortex and in medulla, the total number of nucleated cells within 15 unit areas of 0.017 mm^2 (cortex) and 15 unit areas of 0.034 mm^2 (medulla) was scored.

Analysis of Spleen Sections

GC in spleen sections were analyzed as described (13). The number of precursor cells per GC (m) was calculated on the basis of a binomial distribution as follows: p = proportion of donor cells; $1-p$ = proportion of host cells; p was estimated by the proportion of donor cells in the B lymphoid lineage in BM (Table 3): 0.07 and 0.21 for chimera I and II, respectively. For donor GC, $m = \log_p$ (proportion of donor GC); for host GC, $m = \log_{(1-p)}$ (proportion of host GC). For mixed GC, m was calculated from the formula: 1 − proportion of mixed GC = $p^m + (1-p)^m$.

Results

As reported (34), HIS41 binds exclusively to hemopoietic cells of RT7.2 allotype and not to any cells of 7.1 allotype. In adult BM, <10% of nucleated cells lack detectable levels of the HIS41 antigen. These HIS41$^-$ cells include the more mature stages of erythropoiesis. To assess the usefulness of RT7 allotypes as a genetic marker for hemopoietic cells in our experimental system, we analyzed HIS41 binding to BM cells of RT7^b rats using two-color immunofluorescence on cytospots. The proportion of HIS41$^+$ cells among various nucleated BM cell subpopulations is shown in Table 2. All B lymphoid cells expressed HIS41 as a discrete narrow band around the cells, and virtually all myeloid cells were HIS41$^+$, showing staining more widely spread over the cells. Most erythroid cells bound HIS41, but their HIS41 binding appeared to be derived from adhering macrophage fragments rather than from endogenous HIS41 antigen production (additional data on which this suggestion is based have come from microscopic analysis of HIS49/ED2 double-stained BM cells [not shown]). About 1% of BM nucleated cells were HIS41$^-$ morphologically undifferentiated cells. Their (light) phase contrast morphology indicated that they may include stromal cells. We conclude that the allotypic HIS41 marker is suitable for analysis of lympho-myeloid BM cells, but cannot be used to detect erythroid cells of donor origin in our experimental system.

To construct chimeras (see Materials and Methods), we injected day 14–16 RT7^b FL cells intraperitoneally into 1- or 5-d-old RT7^a rats. All rats injected with FL cells were shown to be chimeric. The cell composition of BM 6–20 wk after injection appeared normal in the chimeras (data not shown). The frequencies of HIS41$^+$ cells in the BM (6–20 wk after injection) of nine chimeras are in Fig. 1. Two rats

Table 2. *HIS41 Binding to BM Cells*

Population	Percentage of all nucleated BM cells	Percentage HIS41$^+$
All nucleated BM cells	100*	97 ± 1
HIS41$^+$	97 ± 1	100*
HIS49$^+$	32 ± 4	94 ± 1
HIS50$^+$	44 ± 4	100 ± 0
TdT$^+$	5 ± 0	100 ± 0
W3/13$^+$	39 ± 9	99 ± 0
ED2$^+$	36 ± 3	100 ± 0

BM cells of 6-wk-old male RT7^b rats were double stained with HIS41 (anti-RT7^b allotype) and one other antibody, and microscopically analyzed for their HIS41 binding. The results are the mean of three animals; at least 1,000 cells of each population were analyzed.
* By definition.

Published May 1, 1992

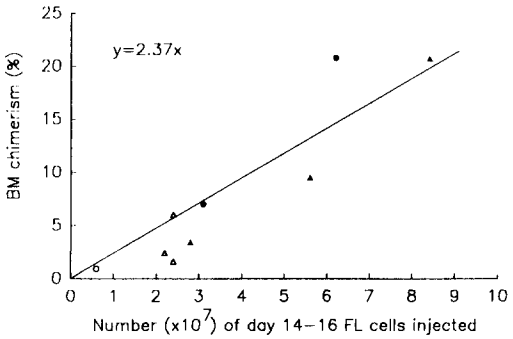

Figure 1. Dose dependency of BM cell chimerism. RT7^a rats were injected with RT7^b FL cells. After 6–20 wk BM was flushed, cell suspensions were stained for donor allotype (HIS41), and microscopically analyzed. BM chimerism = proportion of HIS41$^+$ cells among total nucleated BM cells/(1 − proportion of HIS49$^+$ cells among total nucleated BM cells). (●) Rats injected with RT7^b FL liver cells at day 5 after birth; all others at the day of birth. (△) Analyzed 6 wk after injection; (▲) analyzed 9–10 wk after injection; (○) analyzed 20 wk after injection. The line drawn was forced through zero; gradient nonzero, significance $p < 0.0001$.

were injected at day 5 after birth, and had a degree of chimerism equivalent to rats injected at day 1. There was a linear relationship between the dose of FL cells (x-axis) and the degree of chimerism (percent) at ≥6 wk of age (y-axis). The gradient of the line indicates that for every 4.2 × 10^6 FL cells, there was ~1% more chimerism. We determined the degree of chimerism in various BM subpopulations of three chimeras (Table 3). The extent of chimerism within early or more mature B lymphoid compartments and in the myeloid lineage (defined by W3/13$^+$ plus myeloid morphology) was the same as the overall chimerism among nonerythroid (HIS49$^-$) cells. This shows that, after 6–10 wk, the introduced cells have generated progeny that was as heterogeneous in cell type and developmental stage as host cells.

The Topography of Donor-derived Cells in RT7 Chimeras

The term donor cells refers to donor (RT7^b)-derived HIS41-binding cells.

The BM. Frozen half bones of five 6–10-wk-old chimeras (0.3, 1.6, 2.4, 6.0, and 20.8% chimerism as determined by cytospot analysis of the other half bones) were sectioned completely and double stained with the allotypic marker HIS41 and lineage markers to evaluate the nature and topography of donor cells. Donor B lymphoid (TdT$^+$, μ^+, HIS50$^+$) cells, myeloid (W3/13$^+$) cells, macrophages (ED2$^+$), and megakaryocytes were detected. As expected, none of the erythroid (HIS49$^+$) cells showed HIS41 binding, except for a macrophage-derived patchiness (see Fig. 2 *B*).

Distribution of Donor Cells. Donor cells occurred thoroughly interspersed with HIS41$^-$ cells in all sections (Fig. 2). No areas were found that exclusively contained donor hemopoietic cells. When chimerism was ≥1.6%, donor cells were rather uniformly distributed over the sections (i.e., donor cells were present in all parts of each section in more or less similar relative frequencies). Donor TdT$^+$ and pre-B (weakly μ^+) cells occurred near the bone in higher frequencies than in the center of the marrow, which is normal for precursor B cells (37). The clusters of B lymphocytes in BM sinuses, and the groups of TdT$^+$ and pre-B cells, mostly present in the periphery of the marrow, were never completely or in majority of donor type (Fig. 3).

Although the total (donor plus host) myeloid and lymphoid cells were distributed fully across each transverse marrow section, among the donor cells we saw an uneven distribution. Within a given section, some areas contained considerably more myeloid cells of donor origin than others, and likewise for lymphoid donor cells (Fig. 2). This separation of donor cells into lymphoid and myeloid regions was even more pronounced at low levels of chimerism. In the rat with the lowest chimerism (0.3%; animal excluded from Fig. 1), some areas with only myeloid cells of donor type were found that were spatially separated (two-dimensionally) from areas with only lymphoid cells of donor type.

Number of Active Clones in BM. If marrow cells from one bone develop from small numbers of hemopoietic stem cells, there would be detectable variation in frequency of donor cells between different leg bones of one individual since exchange of cells between different BM sites is minimal (39).

To assess the number of clones that simultaneously contribute to the BM compartment, we judged the quantity of donor cells in different sections from a single bone and in sections from different bones of each chimera. A similar degree of chimerism was found in sections from each of the four leg bones of each individual; within one bone, all sections showed similar degrees of chimerism as well. This was true even for the chimera with the lowest frequency of donor cells (0.3% chimerism). Thus, marrow develops from relatively large numbers of hemopoietic stem cells.

Table 3. *Chimerism in Various BM Populations of RT7 Chimeric Rats*

Population	Percentage HIS41$^+$		
	Chimera I	Chimera II	Chimera III
All nucleated cells	5	14	15
HIS49$^-$	7	21	21
HIS50$^+$	6*	22	22
TdT$^+$	6*	21	18
μ^+	7*	21	24
κ^+	7*	19	21
W3/13^{+} ‡	7	18	22

BM cells from three chimeras, 10 wk after injection of 3.1 × 10^7 day 16 FL cells (I), 6.2 × 10^7 day 16 FL cells (II), and 8.4 × 10^7 day 15 FL cells (III), were double stained for donor allotype (HIS41) and population markers. The percentage of cells expressing HIS41 within the various populations was microscopically determined.

* These data scored 50 double-positive cells; all other data scored 100.

‡ Weakly W3/13$^+$ cells with erythroid phase contrast morphology were not included in this analysis.

Published May 1, 1992

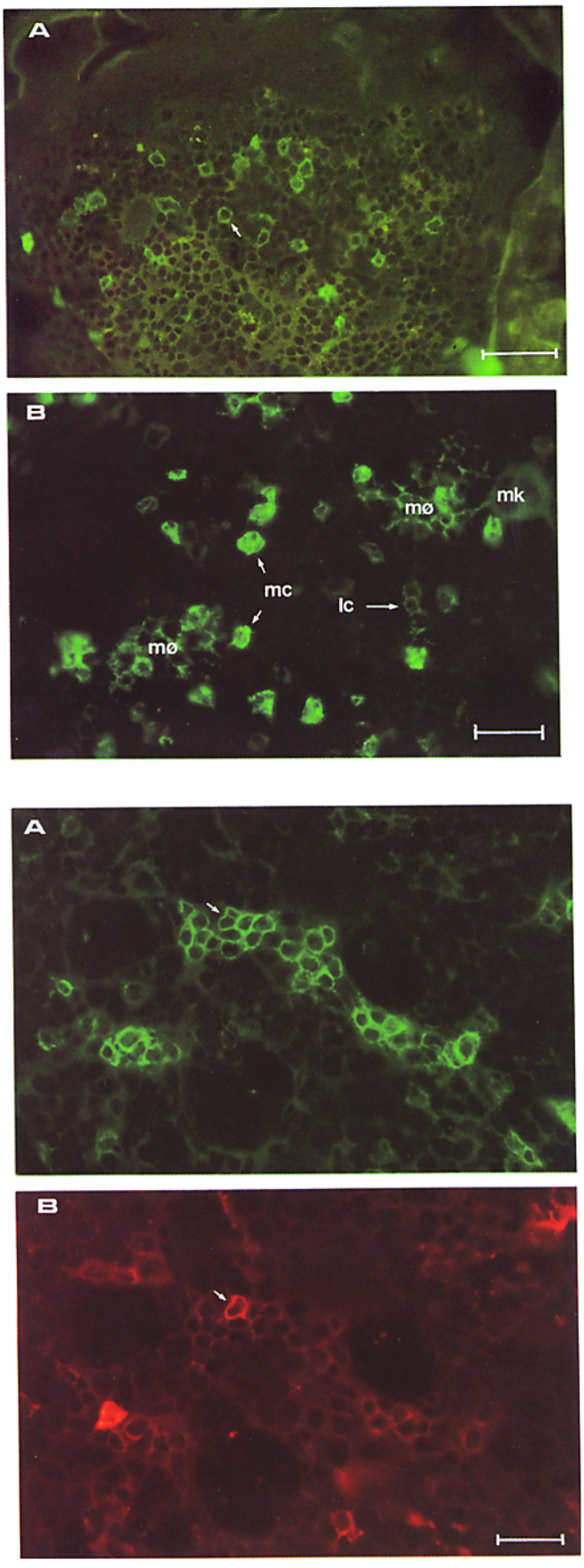

Figure 2. BM of 6-wk-old RT7^a rats injected on the day of birth with 2.2 × 10^7 day 15 (*A*) and 2.4 × 10^7 day 14 (*B*) RT7^b FL cells; BM chimerism of *A* was 2.4%, and of *B* was 6.0%. Cross-sections of frozen femurs were stained for HIS41. (*A*) A subendosteal area of the marrow with virtually only lymphoid donor cells (arrowhead points at example); bar = 25 μm. (*B*) A central area, relatively rich in myeloid donor cells. Lc, lymphoid cell; mϕ, macrophage; mk, megakaryocyte; mc, myeloid cell; bar = 20 μm.

Figure 3. BM section of chimera of Fig. 2 *A* showing a sinus filled with κ$^+$ B lymphocytes. One is donor derived (*arrowhead*). (*A*) Anti-κ and (*B*) HIS41. The strongly TRITC$^+$ cell in the parenchyma (*B*) is a donor myeloid cell; bar = 15 μm.

Germinal Centers. The spleens of two chimeric rats (7% and 21% chimerism in the lymphoid lineage in BM) that had been immunized previously with SRBC were analyzed. Donor cells were randomly distributed over the splenic white pulp, with the exception of GC. We found GC in which either virtually all cells appeared donor derived, virtually none of the cells were donor derived, or in which part of the cells were of donor origin. To evaluate the number of precursor cells that form one GC, we determined the relative frequencies of various types of GC (Table 4). For the calculations of the number of precursor cells per GC, we assumed that each GC arises from a similar number of precursor cells. The numbers of host and mixed-type GC in both chimeras indicated a precursor cell number of 7 or 8, while the number of donor GC in the 21% chimera indicated a precursor cell number of 1.8 (Table 4). We also analyzed part of the spleen of chimera III (Table 4), which was not immunized. Of the seven GC detected, one was of donor type, three were of host type, and three were mixed. Although the number of GC evaluated of the nonimmunized chimera is too low to draw conclusions, there is no indication that these non-SRBC-induced GC had developed from a higher number of precursor cells than SRBC-induced GC.

Thymus. We examined the distribution patterns of donor lymphoid cells in the thymus sections of all nine chimeric rats, stained for HIS41 by immunoperoxidase. HIS41 binds to all $RT7^b$ thymocytes as well as thymic macrophages and interdigitating cells (34). In sections of thymus of chimeric rats, we detected donor cells, practically all of which were lymphoid, although a few were of dendritic morphology. In the following description the data refer to lymphoid cells only. As in BM, the donor lymphoid cells were scattered among host cells. At high chimerism (20%) groups of donor cells were apparent (Fig. 4 *A*). Such groups were absent at lower chimerism (Fig. 4 *B*). In most lobules donor cells were evenly distributed over the lobule cross-section. However, in some lobules (3 out of 24 quantified), a gradient in donor cell proportion was evident.

Quantification of Donor Cell Proportion in Lobules. The thymus of all nine chimeras contained donor cells, with differences in the frequency of donor cells between the various thymic lobules (Fig. 4 *C*). In all thymus sections, donor cells were present in the cortex and medulla of each lobule, except for the two chimeras with the lowest proportion of donor cells. In the thymus section of the 0.9% chimera, all lobules contained donor cells, but one of them had donor cells in the medulla only. Similarly, at 0.3% chimerism, one lobule was found with donor cells in the medulla only, and, in addition, one lobule contained no donor cells at all in the plane of the section. It is most likely that the interlobular differences in donor cell proportions are due to limited numbers of precursor cells per lobule, the extent of variation depending on the number of precursor cells per lobule. Thus, to estimate the number of precursor cells per lobule, we quantified the relative frequencies of donor cells in cortex and medulla of different lobules in a thymus cross-section from two chimeras (the two with ~20% BM·chimerism; Fig. 1). Donor cell frequencies in lobules varied from 9 to 24%. Fig. 5 shows a map of one section with the observed frequencies of donor cells; the complete data are in Tables 5 and 6. There was no strict correlation between donor cell proportion in the cortex and in the medulla of the same lobule. The interlobular differences in cortical donor cell proportion were statistically significant ($p \leqslant 0.0001$), and we analyzed these to estimate the number of cell divisions within the thymus cortex.

Table 4. *RT7 Allotype Composition of GC in Spleen and Calculated Number of Precursor Cells per GC*

	Chimera I		Chimera II	
Type	Percentage	Calculated no. of precursor cells	Percentage	Calculated no. of precursor cells
Host	56	8.0	14	8.3
Mixed	44	8.0	80	6.8
Donor	0	–*	6	1.8

Spleen sections of chimeras I and II (Table 3) were stained for donor cells (HIS41), and at least 100 GC were microscopically analyzed for the presence of donor and/or host cells. Due to the presence of T cells in GC (70), GC with minimal numbers of donor cells were considered to be host type. The number of precursor cells per germinal center was calculated as described in Materials and Methods.
* Cannot be evaluated.

Estimation of the Number of Cell Divisions within the Thymus Cortex. We assumed that (*a*) once present within the thymus, host and donor cells produce progeny to the same extent, and (*b*) all cells within the cortex of a lobule are generated within that lobule. To estimate the number of cell divisions from the interlobular variability in donor cell proportions, we developed (*a*) a mathematical model of cell proliferation in the cortex of a lobule, and (*b*) a corresponding statistical theory (see Appendix). In this model, the total number of thymocytes is constant. Prothymocytes or progeny of intrathymic stem cells enter the dividing compartment in the cortex. The cells that enter are independent of donor or host type with probabilities estimated by the overall frequency of donor and host cells present in the thymus. Each cell that enters divides after one cell cycle time into two cells, then after another cycle time into four cells, and so on. Divisions occur continuously until maturity. The cells then stay in the cortex for a set period of time (a "postmitotic" period), after which they exit the cortical compartment (by cell death or to live on elsewhere). The postmitotic period of rat thymocytes is unknown. In mouse, the postmitotic period for the majority of cortical thymocytes has been estimated to be 3–4 d (40), which is equivalent to about eight cell cycle times (41). The estimate of the number of cell divisions was rather insensitive to the duration of the postmitotic period, but the estimate of the number of cell clones simultaneously contributing to T lymphocyte generation decreased with an increase in postmitotic period (Table 6).

Since serial sections revealed that lobules may vary in size

Published May 1, 1992

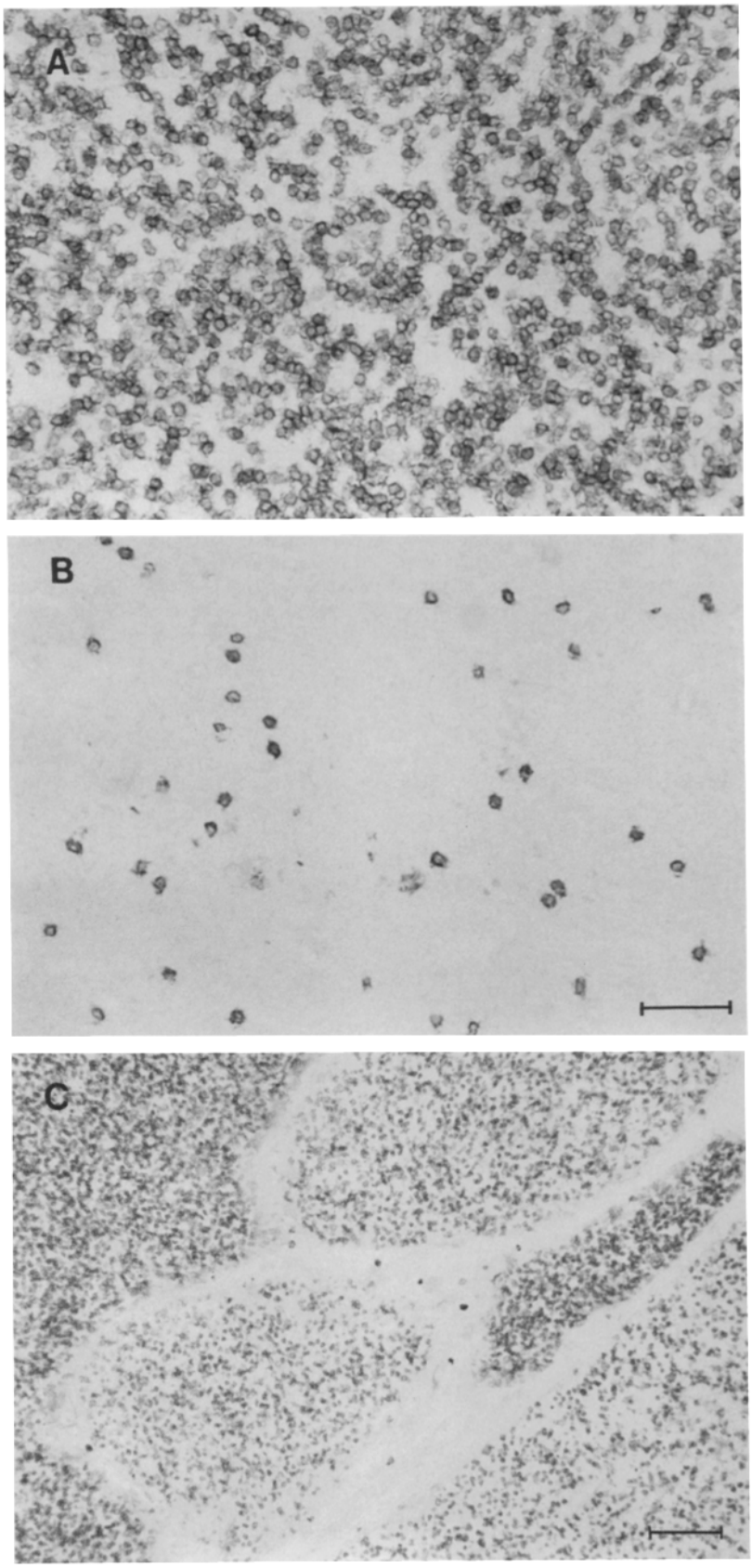

Figure 4. Donor cells in thymus sections of chimeric rats. (*A*) Chimera III (Tables 3 and 5). (*B*) A 20-wk-old $RT7^a$ rat injected with 6×10^6 $RT7^b$ FL cells on the day of birth; BM chimerism was 0.9%; note the degree of dispersion of donor cells; bar = 40 μm (*A* and *B*, same magnification). (*C*) Low-power photograph chimera III; note the variation in donor cell content between different lobules; bar = 100 μm.

Published May 1, 1992

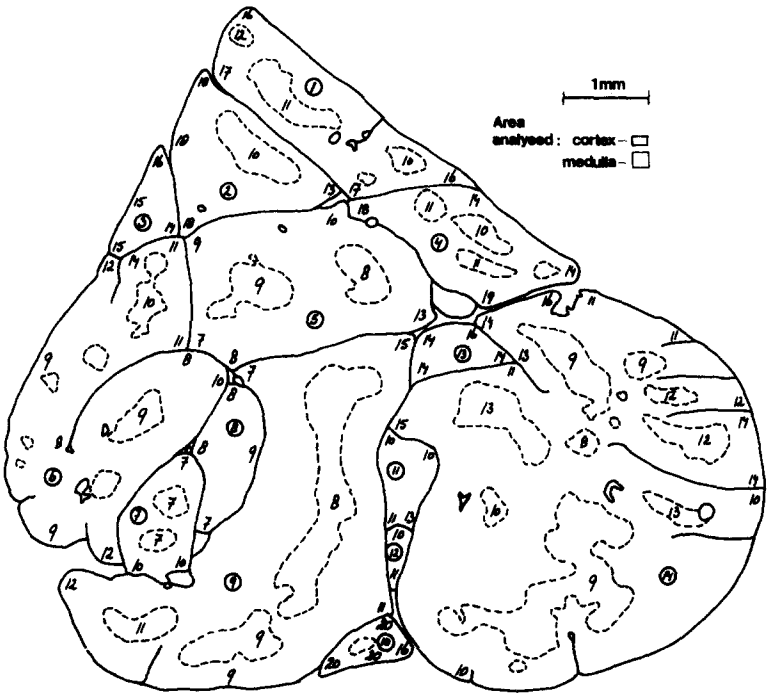

Figure 5. Spatial distribution of donor lymphoid cells in a chimera thymus section. A map of a section of the thymus of chimera II (Tables 3–6), in which the observed frequencies of donor cells (see Materials and Methods) are indicated. Solid lines represent septa or capsule, broken lines demarcate the medulla. Encircled numbers indicate individual lobules, judged to be separate in the plane of sectioning. The two rectangles in the upper right corner represent the surface areas of the samples: 0.017 mm^2 for the cortex and 0.034 mm^2 for the medulla (see Materials and Methods). Note the variation in lobule size and shape, and the absence of a medulla in some. A nonencircled number refers to one in the cortex and at least one in the medulla donor cell frequency determination. Note that there is more variation in cortex donor cell frequencies between different lobules than within a single lobule.

Table 5. *Frequencies of Donor Cells in Different Thymic Lobules*

	Chimera II				Chimera III			
	No. of areas sampled		Average percentage of donor cells		No. of areas sampled		Average percentage of donor cells	
Lobule (i)	cort (r_i)	med	cort ($\bar{y}_i$)	med	cort (r_i)	med	cort ($\bar{y}_i$)	med
1	4	6	16.4	10.8	4		8.7	
2	4	3	16.5	10.3	4	4	11.3	12.4
3	4		15.0		19	20	13.4	10.6
4	4	5	16.1	10.5	2		11.2	
5	5	5	8.8	8.4	2		24.4	
6	10	6	10.5	9.4	2		13.7	
7	3	2	9.1	7.1	4	6	14.7	12.6
8	4		8.0		17	12	11.2	11.6
9	5	10	10.8	9.1	4	2	12.8	11.5
10	4		19.2	10.7	4	2	13.4	12.0
11	4		10.7					
12	2		10.8					
13	4		14.6					
14	12	21	12.5	10.3				

Thymus sections of chimeras II and III (Table 3) were stained for donor cells (HIS41) and photomicrographed. The numbers of (lymphoid) donor cells per unit area in the different lobules were counted on the photographs. The percentage of donor cells = 100 × (HIS41$^+$ cell number per unit area/number of all nucleated cells per unit area), in which the number of all nucleated cells per unit area was 739 ± 35/0.017 mm^2 (15 observations) for the cortex and 773 ± 31/0.034 mm^2 (15 observations) for the medulla.

Published May 1, 1992

Table 6. *Estimation of Number of Cell Divisions in the Cortex*

	Chimera II	Chimera III
Estimated percentage of donor cells ($\hat{\mu}$)	12.6	12.7
Estimated between lobule variance ($\hat{\sigma}^2$)	9.742	6.855
No. of cell divisions in the cortex ($\hat{k}$):		
$d^* = 1$	17.78 ± 0.17	17.27 ± 0.25
$d = 8$	17.31 ± 0.18	16.79 ± 0.24
$d = 100$	17.21 ± 0.18	16.69 ± 0.27
No. of clones within one lobule		
$d = 1$	750	1040
$d = 8$	310	430

BM chimerism of rat II and III was ~21% (Table 3); the lower percentage of donor cells as quantified in these thymus sections is probably due to different methods of analysis. The number of cell divisions in the cortex and the number of clones per lobule were calculated as described in the appendix.
*d = postmitotic period in number of cell cycles, see appendix.

(not shown), we analyzed the sensitivity of our estimate of the number of divisions to plausible variations in size between various lobules (see Appendix). This influence was minimal (less than one division). We conclude that in the thymus cortex of young adult rats, on average 17–18 cell divisions take place between entry and exit, and that at maximum (i.e., a $d = 1$ situation) ~35,000 clones contribute simultaneously to T lymphocyte generation.

Discussion

The interpretations that follow are only valid if we assume that: (*a*) at least some of the FL cells that we introduced into the neonates homed into the BM and had capacity for self-propagation, expansion, and differentiation; (*b*) individual RT7^a and RT7^b progenitor cells in BM, thymus, and GC expand to the same extent in an RT7^a environment, and their progeny disperse similarly; (*c*) the vast majority of lymphoid cells in the structures we analyzed (BM, thymus cortex, and GC) were generated locally.

Evidence for the expansion of the FL cells comes from the presence of relatively high numbers of donor cells in the chimeras 6–20 wk after injection as compared with the number of injected cells. The differentiation ability of the injected cells was shown by the presence of TdT$^+$, pre-B, and B cells in the chimeras, while these cells are absent from day 14–16 FL cells (42, 43, and confirmed in this study). An indication that the donor B lymphoid cells might be derived from self-renewing stem cells was the presence of donor cells of immature phenotype (TdT$^+$ and pre-B cells) up to 20 wk after injection, while the turnover rate of BM B lymphoid cells is high (bromodeoxyuridine labels 85% of the rat BM B lymphoid cells in 3 d; reference 44).

With regard to the second assumption, since the exact function of CD45 and its allelic variants is unknown, we cannot exclude an inequality of RT7^a and RT7^b progenitor cells with regard to cell generation and dispersion of progeny in the chimeric animals. Our observations in BM do not argue against equivalence since the degrees of chimerism found in the myeloid and both early and more mature lymphoid compartments were similar, and the topography of donor B lymphoid cells was normal. Furthermore, RT7^a and RT7^b TDL expand and are functional after transfer to rnu/rnu RT7^a rats (27, 45) without any sign of graft-vs.-host reactivity or any other incompatibility.

With regard to the third assumption, BM, thymus cortex, and GC do contain cells that are likely to be immigrants rather than locally generated (39, 46). However, in BM, immigrant cells form a minor proportion of the total number of cells (47), and in thymus, the vast majority of cortical T lymphoid cells are of the immature T cell phenotype (48, 49), which makes it unlikely that they are immigrant cells. Developing GC contain T lymphocytes, but their number is low (33) and immigration is thought to be minimal (50).

Topography of Donor Cells

Both in BM and thymus, donor cells occurred interspersed with HIS41$^-$ cells. At high degrees of chimerism tight clusters of donor cells were observed. Other workers have observed similar clusters in thymuses and suggested that these represent clones of cells (20). However, such clusters are absent at low chimerism (shown here), and if donor cells were distributed randomly, at a degree of 15% chimerism (used in reference 20), the chance for a donor cell to be part of a two-dimensional cluster of four or more is rather high, ~25% (37). We therefore conclude that cells from one clone do not stay together in groups but disperse upon generation. This rapid dispersion of lymphoid cells has important implications for concepts concerning interactions of cells with microenvironmental elements. As is suggested by the need for particular stromal cells in vitro in B lymphopoiesis, and the necessity of the thymus stroma for T lymphocyte selection, the role of the microenvironment is crucial for certain stages of lymphoid cell differentiation (51, 52). In situ, thymocytes appear to interact with nurse cells, macrophages, and

dendritic cells (20, 55), while the lymphoid progenitors in BM make contact with processes of reticular cells and macrophages (54). The present data suggest that lymphoid progenitor cells do not interact with one particular site of a stromal cell longer than a few divisions, but rather move from one place to the other while differentiating and proliferating. In favor of this concept is the recent observation that at different stages of development, hemopoietic progenitors display different adhesive interactions to fibronectin (55).

Is an In Vivo Clonogenic Assay Feasible? Clonal analysis requires tracing the progeny of one individual stem cell. When the dispersion of progeny is limited, e.g. in the CFU-S assay or in postnatal mouse liver (56) clones remain as discrete colonies, and thus descendants of individual stem cells can be analyzed in situ. In our chimeras the relatively high degree of dispersion of progeny complicates the in situ definition of clones. However, at very low chimerism, the focal accumulations of donor lymphoid or myeloid cells in BM and the absence of donor cells in some lobules of the thymus suggest the feasibility, be it labour-intensive, of such an assay.

Numbers of Clones Contributing to Cell Generation at Any One Time

Bone Marrow. The even distribution of donor cells over the entire marrow, even at low chimerism, fits with a polyclonal maintenance of BM lymphoid and myeloid compartments and is in agreement with other reports on hemopoiesis in nonirradiated rodents (6, 7).

Germinal Centers. We found the most inhomogeneous distribution of cells of the two genotypes within the GC in the spleen. SRBC-induced GC appeared to be generated from about seven precursors. The evaluation of GC as to whether they were host or mixed type was complicated by the presumed presence of T cells in the GC. We have arbitrarily set a boundary. If this boundary were set too high, the number of precursor cells we calculated from the observed frequency of mixed and host type GC would be too low, and vice versa. The large deviation of the number of precursor cells calculated on the basis of the frequency of donor type GC in chimera II from the numbers based on the frequency of mixed and host type GC (1.8 vs. 7–8) may indicate that our assumption that all GC have the same number of precursor cells was wrong and that, consequently, GC may develop from variable numbers of precursor cells.

Our findings confirm that GC may develop oligoclonally as reported (12–14), but may conflict with a report on allophenic rats (18), stating absence of evidence for mono- or oligoclonal development of GC in the spleen. With the limited information presented there, the reason for this remains unclear.

Thymus. In all chimeric thymusses, donor cells were thoroughly interspersed with host cells. This apparently conflicts with data on the thymus of allophenic rats with two MHC haplotypes that showed rather large patches of either MHC class I haplotype (18). An oligoclonal composition of thymocytes under physiological conditions was concluded from this pattern. However, both epithelial cells and lymphoid cells in cortex and medulla express class I. In rat thymic sections, most of class I staining in the cortex is derived from epithelial cells (50). Possibly, therefore, the observations in the Weinberg et al. (18) study referred to the genesis of epithelium rather than of thymocytes. In addition, MHC is involved in selection processes of subpopulations within the thymus (57), and may consequently not be the most suitable chimeric marker for studying clonal development of thymocytes.

We quantified donor cell frequencies in different lobules and developed a mathematical model to estimate the number of cell divisions between entry into and exit from the cortex from these data. The result was 17–18 cell divisions. Since cell proliferation in the medulla is minimal (58), this can be viewed as an estimate for the total number of cell divisions in the thymus. This agrees very well with an estimation of the expansion of prethymic progenitors in the mouse thymus (10^5 = 16–17 divisions) by Shortman et al. (59), based on reconstitution experiments after irradiation. Our data (Table 5) indicate that in young adult rats thymopoiesis is highly polyclonal, with a maximum of ~30,000 clones simultaneously engaged in cell generation. Rough estimates in mouse are of the order of hundreds (59).

In the calculations we assume that lobule sizes are constant and that all cells present in one lobule are generated within that lobule. A three-dimensional reconstruction of the rat thymus has shown that the interlobular septa form an irregular network of walls that divide a lobe into lobules, variable in size, which may or may not interconnect with other lobules (60). Therefore, first, lobules have different sizes, and second, exchange of cells between some individual lobules is likely to occur. A mathematical test of whether differences in size among lobules affected the number of cell divisions obtained from our data showed that lobule size mattered little. The interconnection between lobules implies that progenitor T cells from one lobule may contribute to progeny in other lobules as well, so that we probably underestimate the true number of cell divisions, depending on the extent of cell exchange between lobules.

Since the kinetics of T lymphoid cell clones are unknown and little is known about the self-renewing capacity and propagative behavior of thymic progenitors under normal physiological conditions, different models for the generation of thymocytes can be proposed. Other workers have used a binomial model to estimate the number of prothymocytes reconstituting the thymus after irradiation (16). Their model assumes constant clone sizes, which implies that no division occurs (k = 0 in our model), or, alternatively, the existence of a fixed population of intrathymic stem cells that continuously produce progeny without new prothymocytes entering the thymus. Application of the binomial model to our data estimates the number of cell divisions to be 16 and the number of clones simultaneously active in one lobule to be 130. However, our model is more suitable since it takes into account the dynamics of prothymocytes and/or intrathymic stem cells. Support for our model came from observations at low chimerism where lobules were seen that contained donor cells in the medulla only. This suggests (if medullary cells are derived from cortical cells) that production of thymocytes by

Published May 1, 1992

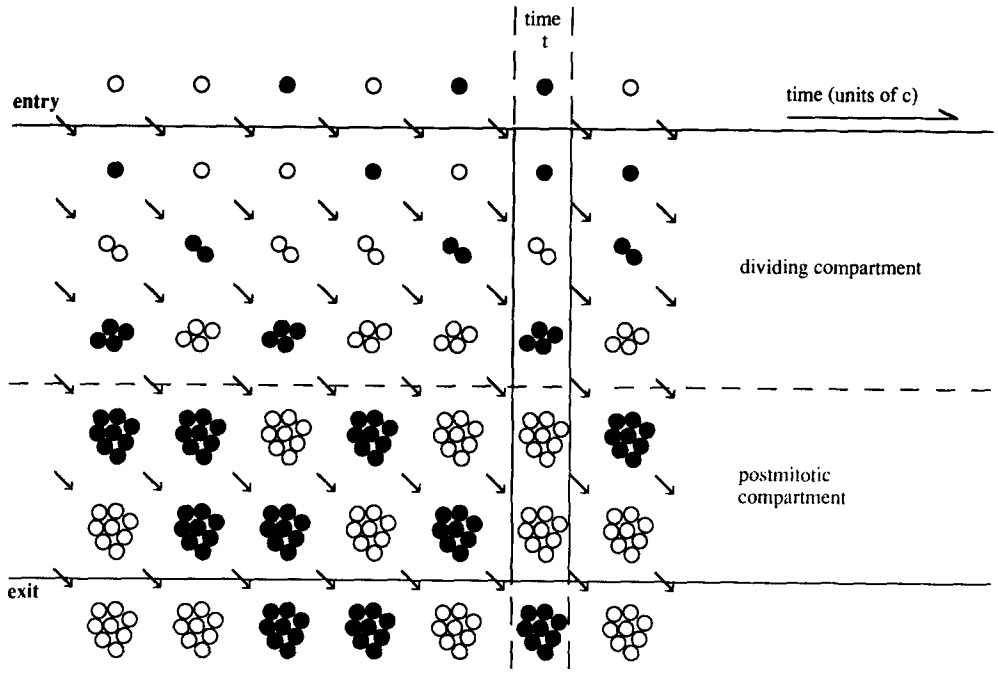

Figure 6. Diagram to illustrate the mathematical model of T lymphoid cell generation in the thymus cortex. Every time c, one cell (a prothymocyte or a progeny cell of an intrathymic stem cell) enters the dividing compartment of the cortex, dividing every time c to give one wave of proliferation of cells. After 3 c, no further divisions take place and the cells enter the postmitotic compartment. They stay in this compartment for another 2 c, after which they leave the thymus cortex.

a single precursor occurs in waves (as in Figure 6) rather than continuously.

Studies on cell population dynamics indicate that a considerable imbalance exists between cell production in and exit from the thymus (61). Cells without productive TCR gene rearrangements may die, and positive and negative selections are thought to take place in the thymus (for reviews see references 62 and 63). To date there is no consensus with regard to the stages of development of T lymphocytes at which the various selective forces operate. In nontransgenic animals, both positive and negative selection seem to occur rather late in the development of T lymphocytes, appearing during and/or after transition from the double-positive stage to the single-positive stage (57, 64, 65). Of the cells that (presumably) die in the thymus, at least part appear to have postmitotic periods in the double-positive compartment of the thymus similar to those of the cells that undergo further maturation (41). Since our mathematical model permits such imbalance in the late, postmitotic stage, our estimate of the number of cell divisions in the cortex will hardly be influenced by these processes. Loss of cells earlier in development may influence the correctness of our estimate, depending on the impact of deletion on the clonal composition of the thymus. The interlobular variation in donor cell proportions in the medulla was less than in the cortex. If medullary cells derive from cortical cells, this indicates that fluctuations in donor cell content are quenched. Possible explanations might include: a relatively long transit time through mature (medullary) T lymphocyte compartments as compared with the earlier (cortical) compartments; or that the exit from the medullary compartments is random rather than "first in first out," as appears to be the case in the postmitotic $CD4^+$ $CD8^+$ compartment (59). Other quenching influences could be interlobular exchange of medullary cells and/or the traffic of circulating B and T lymphocytes through the medulla (66–68).

Our in situ analysis of donor cells in nonradiation chimeras has brought forward three important aspects of lymphocyte development. (*a*) Progeny cells disperse rapidly, suggesting that the lymphohemopoietic microenvironment must be viewed in highly dynamic terms. (*b*) In young adult rats both early B and T lymphocytopoiesis are polyclonal, allowing the generation and maintenance of a population highly diverse in antigen-receptor repertoire, even with relatively early commitments of its individuals to the use of certain variable region gene segments. (*c*) In situ definition of lymphoid cell clones seems feasible. Detection of antigen receptor gene usage within such clones will reveal the impact of the timing of commitments on repertoire generation.

Appendix

Mathematical Estimation of Number of Cell Divisions within the Thymus Cortex

We observed that some lobules contained considerably more donor cells than other lobules. If thymic precursor cells divide a certain number of times, such differences originate. To translate the interlobular differences in donor cell proportions into the number of cell divisions, we needed a mathematical model of cell proliferation in the thymus.

Mathematical Model. We have developed a mathematical model in which cells divide within a "compartment with fixed capacity" (the lobule cortex). Cells entering the compartment are independent of donor type with probability (p), or of host type with probability (1-p). Each cell that enters

Published May 1, 1992

divides after a cycle time (c) into two cells, then into four cells at time 2 c, and so on; divisions occur after each time period c until maturity. We assume no variation in cell cycle time. There are k cell divisions, so each entering cell develops into 2^k mature cells. We assume that these cells leave a "dividing" compartment after a period kc, to enter a "non-dividing" (postmitotic) compartment where they stay for time dc. Their disappearance at time $(k+d)c$ creates space for the entry of one new cell and the division of 2^k-1 other cells. The new cell may come from outside the thymus, or alternatively from division of an intrathymic stem cell. The scheme is illustrated for $k = 3$ and $d = 2$ in Fig. 6, where a stable number of 23 cells (in general $[d+1]2^k-1$) is maintained in the compartment. We then generalize this to permit the existence of many independent groups of size $(d+1)2^k-1$, each operating in the manner of Fig. 6, though possibly asynchronously. Thus, the total number of cells (N) in the compartment is: $N = g[(d+1)2^k-1]$ (Eq. 1); where g is the number of groups. The expectation and variance of N^+, the number of donor cells, are: $E(N^+) = pg[(d+1)2^k-1]$ and Var $(N^+) = p(1\text{-}p)g\ [(4^{k+1}-1)/3+(d-1)4^k]$ (Eq. 2).

The rationale behind the variance formula above is easily seen from the example in Fig. 6 where $k = 3$, $d = 2$, and $g = 1$. At observation time t, N comprises five clones, each one of which may be independently donor type with probability p. Thus, $N^+ = X_0 + 2X_1 + 2^2X_2 + 2^3X_3 + 2^3X_4$ where each quantity X is, randomly, equal to either 1 with probability p or 0 with probability 1-p. Hence, the variance of the X quantities is p(1-p), and $\text{Var}(N^+) = 1^2\text{Var}(X_0) + 2^2\text{Var}(X_1) + 2^4\text{Var}(X_2) + 2^6\text{Var}(X_3) + 2^6\text{Var}(X_4) = p(1-p)[1+4+4^2+4^3+4^3] = p(1-p)[(4^4-1)/3+4^3]$.

Our experimental method measures the proportion of donor cells, namely N^+/N. We have that $E\ (N^+/N) = p$, while Var $(N^+/N) = [\text{Var}\ (N^+)]/N^2$, which we write in terms of k and N, using $g = N/[(d + 1)2^k-1]$ from Eq. 1. Thus, if we denote $E(N^+/N)$ by μ and Var (N^+/N) by σ^2, we have: $\mu = p$, $\sigma^2 = p(1-p)[(3d+1)4^k-1]/3N[(d+1)2^k-1]$ (Eq. 3). The sample mean estimates μ and the sample variance estimates σ^2. Given values of N and d, k can be found from Eq. 3 (see below).

Statistical Analysis. This section deals with statistical issues in the estimation of μ and σ^2 for use in Eq. 3. We have taken replicate observations for each lobule (r_i readings in lobule i). Assuming that the n different lobules have a common p, d, N, and k, we apportioned the total variance into "between" and "within" lobule variance using standard methods of analysis of variance (69), and took the between lobule variance as the σ^2 to estimate k. The usual unbiassed estimator of σ^2 is: $\hat{\sigma}^2 = R[\Sigma_i r_i(\bar{y}_i-\bar{y})^2 - (n-1)\ \Sigma_{ij}\ (y_{ij}-\bar{y}_i)^2/(R-n)]/\ R^2 - \Sigma_i r_i^2$. Here, R is the total sample size (i.e., $\Sigma\ r_i$), y_{ij} is the j^{th} sample value in lobule i ($i = 1, 2, \ldots n$; $j = 1,2, \ldots r_i$), $\bar{y}_i$ is the mean of the r_i values in lobule i, and $\bar{y}$ is the overall mean ($\Sigma_i r_i\bar{y}_i/R$). The estimator of μ is $\bar{y}$. Results of this statistical estimation for chimeras II and III are shown as $\hat{\mu}$ and $\hat{\sigma}^2$ (Table 6).

Estimation of k. Given estimates $\hat{\mu}$ and $\hat{\sigma}^2$, k is found via the solution of Eq. 3, provided there is information about N and d. N was estimated as follows: a whole thymus of a 10-wk-old, unstressed, normally reared rat contains $\sim 8 \times 10^8$ lymphocytes (H. Groen, personal communication) divided over $\sim$40 lobules, 20 in each lobe (estimated from Sainte-Marie's data [60] and our data [not shown] on cross-sections of a whole thymus). About 85% of thymic lymphocytes are located in the cortex (49). Thus, on average a lobule contains 17×10^6 cortical lymphocytes. As a first calculation, we used this average N value as a common N value. We do not know d. Trying an extensive range of d values, we found that the resulting estimate $\hat{k}$ was not very sensitive to the choice of d. Table 6 shows $\hat{k}$ for a range of d, together with standard errors resulting from the variation in readings within a lobule.

The number of clones per lobule is equal to g (the number of groups per lobule: $d = 1$, 38 and 54; $d = 8$, 12 and 17, for thymus II and III, respectively) times the number of clones per group ($= k + d + 1$).

Sensitivity Analysis. Our estimate of k is insensitive, within biological accuracy, to changes in d. So our ignorance of d is unimportant. Also a 10% error in our estimate of a common N gives $\hat{k}$ values very close to those in Table 6 (within 0.15 of a generation). Another concern was our assumption of a common N value (all lobules have the same size). We therefore modified the earlier statistical analysis to obtain a method for estimating k in case N varies from lobule to lobule (details omitted here, but available on request). We then analyzed the sensitivity of $\hat{k}$ by taking numerous plausible sets of unequal N values having the same average as in our first calculation (17×10^6). The $\hat{k}$ value was fairly insensitive to these changes in the N values (ranging from 2×10^6 to 44×10^6 across lobules, $d = 1$) resulting in the number of cell divisions ($\hat{k}$) changing from 17.8 (thymus II) to 17.0. If we suppose that the 14 lobules measured were larger than average by 30% (i.e., stereological bias toward cutting the bigger lobules), the number of cell divisions changed from 17.8 to 18.2.

In summary, the cell division number of 17–18 is quite an accurate estimation, and a true cell division number of, let us say, 15 would be highly unlikely. However, since the exchange of cells between the different compartments is unknown and assumed to be zero, the true number of cell divisions could be slightly higher than 17–18.

We thank Ken Shortman for a very helpful discussion; Pierre Golstein, Paul Kincade, and Paul Nieuwenhuis for invaluable critical comments; Nienke de Boer, Jaap Kampinga, and Bruce Roser for supply of RT7 chimeras for our pilot study; Wim Ammerlaan for technical assistance; and the Department of Anatomy, University of Hong Kong, for use of microscopes.

This work was supported by grants from the Dutch Foundation for Medical and Health Research MEDIGON, which is subsidized by the Netherlands Organization for Scientific Research (NWO 900-105-125), the J. K. de Cock Stichting (Groningen, the Netherlands), the Committee on Research and Conference Grants, the Medical Faculty Research Grant Fund (The University of Hong Kong), the Croucher Foundation, Hong Kong, and La Fondation pour la Recherche Medicale (France).

Address correspondence to Mirjam H.A. Hermans, Centre d'Immunologie, INSERM/CNRS de Marseille-Luminy, Case 906, 13288 Marseille Cedex 9, France.

Received for publication 24 May 1991 and in revised form 21 January 1992.

References

1. Barnes, D.W.H., C.E. Ford, S.M. Gray, and J.F. Loutit. 1959. Spontaneous and induced changes in cell populations in heavily irradiated mice. *Prog. Nucl. Energy, Ser. VI.* 2:1.
2. Keller, G., C. Paige, E. Gilboa, and E.F. Wagner. 1985. Expression of a foreign gene in myeloid and lymphoid cells derived from multipotent haematopoietic precursors. *Nature (Lond.).* 318:149.
3. Micklem, H.S., J.E. Lennon, J.D. Ansell, and R.A. Gray. 1987. Numbers and dispersion of repopulating hematopoietic cell clones in radiation chimeras as functions of injected cell dose. *Exp. Hematol.* 15:251.
4. Capel, B., R. Hawley, L. Covarrubias, T. Hawley, and B. Mintz. 1989. Clonal contributions of small numbers of retrovirally marked hemopoietic stem cells engrafted in unirradiated neonatal W/W^v mice. *Proc. Natl. Acad. Sci. USA.* 86:4564.
5. Smith, L.G., I.L. Weissman, and S. Heimfeld. 1991. Clonal analysis of hematopoietic stem-cell differentiation in vivo. *Proc. Natl. Acad. Sci. USA.* 88:2788.
6. Behringer, R.R., P.W. Eldridge, and M.J. Dewey. 1984. Stable genotypic composition of blood cells in allophenic mice derived from congenic C57BL/6 strains. *Dev. Biol.* 101:251.
7. Harrison, D.E., C. Lerner, P.C. Hoppe, G.A. Carlson, and D. Alling. 1987. Large numbers of primitive stem cells are active simultaneously in aggregated embryo chimeric mice. *Blood.* 69:773.
8. Lemischka, I.R., D.H. Raulet, and R.C. Mulligan. 1986. Developmental potential and dynamic behavior of heamopoietic stem cells. *Cell.* 45:917.
9. Keller, G., and R. Snodgrass. 1990. Life span of multipotential hematopoietic stem cells in vivo. *J. Exp. Med.* 171:1407.
10. Jordan, C.T., and I.R. Lemischka. 1990. Clonal and systemic analysis of long-term hematopoiesis in the mouse. *Genes & Dev.* 4:220.
11. Capel, B., R.G. Hawley, and B. Mintz. 1990. Long- and short-lived murine hematopoietic stem cell clones individually identified with retroviral integration markers. *Blood.* 75:2267.
12. MacLennan, I.C.M., Y.J. Liu, S. Oldfield, J. Zhang, and P.J.I. Lane. 1990. The evolution of B-cell clones. *Curr. Top. Microbiol. Immunol.* 159:37.
13. Kroese, F.G.M., A.S. Wubbena, H.G. Seijen, and P. Nieuwenhuis. 1987. Germinal centers develop oligoclonally. *Eur. J. Immunol.* 17:1069.
14. Jacob, J., R. Kassir, and G. Kelsoe. 1991. In situ studies of the primary immune response to (4-hydroxy-3-nitrophenyl) acetyl. I. The architecture and dynamics of responding cell populations. *J. Exp. Med.* 173:1165.
15. Moore, M.A.S., and J.J.T. Owen. 1967. Experimental studies on the development of the thymus. *J. Exp. Med.* 126:715.
16. Wallis, V.J., E. Leuchars, S. Chwalinski, and A.J.S. Davies. 1975. On the sparse seeding of bone marrow and thymus in radiation chimaeras. *Transplantation (Baltimore).* 19:2.
17. Ezine, S., I.L. Weissman, and R.V. Rouse. 1984. Bone marrow cells give rise to distinct cell clones within the thymus. *Nature (Lond.).* 309:629.
18. Weinberg, W.C., J.C. Howard, and P.M. Iannaccone. 1985. Histological demonstration of mosaicism in a series of chimeric rats produced between congenic strains. *Science (Wash. DC).* 227:524.
19. Iannaccone, P.M. 1987. The study of mammalian organogenesis by mosaic pattern analysis. *Cell Differ.* 21:79.
20. Kyewski, B.A. 1987. Seeding of thymic microenvironments defined by distinct thymocyte-stromal cell interactions is developmentally controlled. *J. Exp. Med.* 166:520.
21. Fleishman, R.A., and B. Mintz. 1984. Development of adult bone marrow stem cells in H-2-compatible and incompatible mouse fetuses. *J. Exp. Med.* 159:731.
22. Micklem, H.S., C.E. Ford, E.P. Evans, D.A. Ogden, and D.S. Papworth. 1972. Competitive in vivo proliferation of foetal and adult haematopoietic cells in lethally irradiated mice. *J. Cell. Physiol.* 79:293.
23. Thomas, D.B., C.M. Smith, and J.M. Sumpster. 1976. The proliferation of transplanted haemoatopoietic cells derived from bone marrow and fetal liver. *J. Anat.* 122:15.
24. Hunt, S.V., and M.H. Fowler. 1981. A repopulation assay for B and T lymphocyte stem cells employing irradiation chimaeras. *Cell Tissue Kinet.* 14:445.
25. Jordan, C.T., J.P. McKearn, and I.R. Lemischka. 1990. Cellular and developmental properties of fetal hematopoietic stem cells. *Cell.* 61:953.
26. Sunderland, C.A., W.R. McMaster, and A.F. Williams. 1979. Purification with monoclonal antibody of a predominant leukocyte-common antigen and glycoprotein from rat thymocytes. *Eur. J. Immunol.* 9:155.
27. Bell, E.B., S.M. Sparshott, M.T. Drayson, and S.V. Hunt. 1989. The origin of T cells in permanently reconstituted old athymic nude rats. Analysis using chromosome or allotype markers. *Immunology.* 68:547.
28. Lubaroff, D.M. 1973. An alloantigenic marker on rat thymus and thymus-derived cells. *Transplant. Proc.* 5:115.
29. Williams, A.F. 1975. IgG2 and other immunoglobulin classes on the cell surface of rat lymphoid cells. *Eur. J. Immunol.* 5:883.
30. Williams, A.F., G. Galfrè, and C. Milstein. 1977. Analysis of cell surfaces by xenogeneic myeloma-hybrid antibodies: differentiation antigens of rat lymphocytes. *Cell.* 12:663.
31. Dijkstra, C.D., E.A. Dopp, P. Joling, and G. Kraal. 1985. The heterogeneity of mononuclear phagocytes in lymphoid organs:

distinct macrophage subpopulations in the rat recognized by monoclonal antibodies ED1, ED2, and ED3. *Immunology.* 54:589.
32. Deenen, G.J., S.V. Hunt and D. Opstelten. 1987. A stathmokinetic study of B-lymphocytopoiesis in rat bone marrow: proliferation of cells containing cytoplasmic μ chains, terminal deoxynucleotidyl transferase and carrying HIS24 antigen (1). *J. Immunol.* 139:702.
33. Kroese, F.G.M., D. Opstelten, A.S. Wubbena, G.J. Deenen, J. Aten, E.H. Schwander, L. de Ley, and P. Nieuwenhuis. 1985. Monoclonal antibodies to rat B lymphocyte (sub-)populations. *Adv. Exp. Med. Biol.* 186:81.
34. Kampinga, J., F.G.M. Kroese, G.H. Pol, D. Opstelten, H.G. Seijen, J.H.A. Boot, B. Roser, P. Nieuwenhuis, and R. Aspinall. 1990. RT7-defined alloantigens in rats are part of the leucocyte common antigen family. *Scand. J. Immunol.* 31:699.
35. Hermans, M.H.A., and D. Opstelten. 1991. In situ visualization of hemopoietic cell subsets and stromal elements in rat and mouse bone marrow by immunostaining of frozen sections. *J. Histochem. Cytochem.* 39:1627.
36. Opstelten, D., G.J. Deenen, J. Rozing, and S.V. Hunt. 1986. B lymphocyte-associated antigens on terminal deoxynucleotidyl transferase-positive cells and pre-B cells in bone marrow of the rat. *J. Immunol.* 137:76.
37. Hermans, M.H.A., H. Hartsuiker, and D. Opstelten. 1989. An in situ study of B-lymphocytopoiesis in rat bone marrow: topographical arrangement of terminal deoxynucleotidyl transferase-positive cells and pre-B cells. *J. Immunol.* 142:67.
38. Kroese, F.G.M., A.S. Wubbena, D. Opstelten, G.J. Deenen, E.H. Schwander, L. de Leij, H. Vos, S. Poppema, J. Volberda, and P. Nieuwenhuis. 1987. B lymphocyte differentiation in the rat: production and characterization of monoclonal antibodies to B lineage associated antigens. *Eur. J. Immunol.* 17:921.
39. Harris, J.E., C.E. Ford, D.W.H. Barnes, and E.P. Evans. 1964. Cellular traffic of the thymus: experiments with chromosome markers. Evidence from parabiosis for an afferent stream of cells. *Nature (Lond.).* 201:886.
40. Shortman, K., D. Vremec, M. Egerton. 1990. The kinetics of T cell antigen receptor expression by subgroups of $CD4^+8^+$ thymocytes: delineation of $CD4^+8^+3^{2+}$ thymocytes as post-selection intermediates leading to mature T cells. *J. Exp. Med.* 173:323.
41. Penit, C. 1986. In vivo thymocyte maturation, BUdR labeling of cycling thymocytes and phenotypic analysis of their progeny support the single lineage model. *J. Immunol.* 137:2155.
42. Gregoire, K.E., I. Goldschneider, R.W. Barton, and F.J. Bollum. 1979. Ontogeny of terminal deoxynucleotidyl-positive cells in lymphohemopoietic tissues of rat and mouse. *J. Immunol.* 123:1347.
43. Veldhuis, G.J., and D. Opstelten. 1989. B cell precursor populations in fetal and neonatal rat liver: frequency, topography and antigenic phenotype. *Adv. Exp. Med. Biol.* 237:57.
44. Deenen, G.J., I. Van Balen, and D. Opstelten. 1990. In rat B lymphocyte genesis sixty percent is lost from the bone marrow at the transition of nondividing pre-B cell to $sIgM^+$ B lymphocyte, the stage of Ig light chain gene expression. *Eur. J. Immunol.* 20:557.
45. Bell, E.B., and S.M. Sparshott. 1990. Interconversion of CD45R subsets of CD4 T cells in vivo. *Nature (Lond.).* 348:163.
46. Gutman, G.A., and I.L. Weissman. 1972. Lymphoid tissue architecture. Experimental analysis of the origin and distribution of T cells and B cells. *Immunology.* 23:465.
47. Westermann, J., S. Ronneberg, F.J. Fritz, and R. Pabst. 1989. Proliferation of lymphocyte subsets in the adult rat: a comparison of different lymphoid organs. *Eur. J. Immunol.* 19:1087.
48. Van Ewijk, W., P.L. van Soest, and G.J. van den Engh. 1981. Fluorescence analysis and anatomical distribution of mouse T lymphocyte subsets defined by monoclonal antibodies to the antigens Thy-1, Lyt-1, Lyt-2, and T-200. *J. Immunol.* 127:2594.
49. Paterson, D.J., J.R. Green, W.A. Jefferies, M. Puklavec, and A.F. Williams. 1987. The MRC OX-44 antigen marks functionally relevant subset among rat thymocytes. *J. Exp. Med.* 165:1.
50. Pellas, T.C., and L. Weiss. 1990. Migration pathways of recirculating murine B cells and $CD4^+$ and $CD8^+$ T lymphocytes. *Am. J. Anat.* 187:355.
51. Kincade, P.W., G. Lee, C.E. Pietrangeli, S.I. Hayashi, and J.M. Gimble. 1989. Cells and molecules that regulate B lymphopoiesis in bone marrow. *Annu. Rev. Immunol.* 7:111.
52. Fry, A.M., L.A. Jones, A.M. Kruisbeek, and L.A. Matis. 1989. Thymic requirement for clonal deletion during T cell development. *Science (Wash. DC).* 246:1044.
53. Wekerle, H., U.P. Ketelsen, and M. Ernst. 1980. Thymic nurse cells. Lymphoepithelial complexes in murine thymus: morphological and serological characterization. *J. Exp. Med.* 151:925.
54. Jacobsen, K., and D.G. Osmond. 1990. In vivo localization of B lymphocyte precursor cells and stromal cell associations in mouse bone marrow. *Eur. J. Immunol.* 20:2395.
55. Verfaillie, C.M., J.B. McCarthy, and P.B. McGlave. 1991. Differentiation of primitive human multipotent hematopoietic progenitors into single lineage clonogenic progenitors is accompanied by alterations in their interaction with fibronectin. *J. Exp. Med.* 174:693.
56. Rossant, J., K.M. Vijh, C.E. Grossi, and M.D. Cooper. 1986. Clonal origin of haematopoietic colonies in the postnatal mouse liver. *Nature (Lond.).* 319:507.
57. Benoist, C., and D. Mathis. 1989. Positive selection of the T cell repertoire: where and when does it occur? *Cell.* 58:1027.
58. Penit, C. 1986. In vivo thymocyte maturation. BUdR labeling of cycling thymocytes and phenotypic analysis of their progeny support a single lineage model. *J. Immunol.* 137:2115.
59. Shortman, K., M. Egerton, G.J. Spangrude, and R. Scollay. 1990. The generation and fate of thymocytes. *Semin. Immunol.* 2:3.
60. Sainte-Marie, G. 1974. Tridimensional reconstruction of the rat thymus. *Anat. Rec.* 179:517.
61. Scollay, R.G., E.C. Butcher, and I.L. Weissman. 1980. Thymus cell migration. Quantitative aspects of cellular traffic from the thymus to the periphery in mice. *Eur. J. Immunol.* 10:210.
62. Schwarz, R.H. 1989. Acquisition of immunologic self-tolerance. *Cell.* 57:1073.
63. von Boehmer, H. 1990. Developmental biology of T cells in T cell-receptor transgenic mice. *Annu. Rev. Immunol.* 8:531.
64. Hengartner, H., B. Odermatt, R. Schneider, M. Schreyer, G. Walle, H.R. MacDonald, and R.M. Zinkernagel. 1988. Deletion of self-reactive T cells before entry into the thymus medulla. *Nature (Lond.).* 336:388.
65. Guidos, C.J., J.S. Danska, C.G. Garrison Fathman, and I.L. Weissman. 1990. T cell receptor-mediated negative selection of autoreactive T lymphocyte precursors occurs after commitment to the CD4 or CD8 lineages. *J. Exp. Med.* 172:835.
66. Fink, P.J., M.J. Bevan, and I.L. Weissman. 1984. Thymic cytotoxic T lymphocytes are primed in vivo to minor histocompatibility antigens. *J. Exp. Med.* 159:436.
67. Hirokawa, K., M. Utsuyama, and T. Sado. 1989. Immunohistological analysis of immigration of thymocyte-precursors

into the thymus: evidence for immigration of peripheral T cells into the thymic medulla. *Cell. Immunol.* 119:160.
68. Hwang, W.S., T.Y. Ho, S.C. Luk, G.T. Simon. 1974. Ultrastructure of the rat thymus. A transmission, scanning electron microscope, and morphometric study. *Lab. Invest.* 31:473.
69. Graybill, F.A. 1961. An Introduction to Linear Statistical Models. McCraw-Hill Inc., New York. 351 pp.
70. Kroese, F.G.M., A.S. Wubbena, P. Joling, and P. Nieuwenhuis. 1985. T lymphocytes in rat lymphoid follicles are a subset of T helper cells. *Adv. Exp. Med. Biol.* 186:443.